Scanning Microwave Microscopy of Active Superconducting Microwave Devices

Steven M. Anlage, C. P. Vlahacos, Sudeep Dutta, and F. C. Wellstood
Center for Superconductivity Research, Physics Department, University of Maryland, College Park, MD 20742-4111

Abstract -- We have developed a scanning microwave microscope which can image features with 20 μm spatial resolution. The microscope consists of a section of open-ended coaxial cable which is scanned over the surface of a planar sample. Images can be made in either passive mode, in which the reflectivity of the probe tip is measured as a function of position, or in active mode, in which stray fields from the sample are picked up by the scanning probe and measured with a vector demodulation circuit. We have imaged reflectivity variations of metallic and superconducting samples in passive mode to determine the spatial resolution of the technique. Images are also presented in active mode of a superconducting microwave device taken at liquid nitrogen temperature.

I. Introduction

Non-linearity, intermodulation and power dependence are problems of crucial importance in applying high-T_c superconductors to microwave communications circuits. Innovative approaches are required to understand the causes of power dependence and nonlinearity in superconducting microwave devices. Our approach is to directly image the microwave fields in active devices to better understand the microscopic origins of nonlinearity. To do this, it is necessary to image microwave signals on length scales much less than the free space or guided wavelength of the radiation. This requires the use of near-field microscopy techniques, which were originally pioneered in the microwave range [1]. Once this is accomplished, one can image the microwave fields in an active circuit while it is in operation, and correlate the overall performance with specific local microstructure and device geometry features.

II. Experiment

Scanning coaxial microwave microscopes have been used by a number of researchers to passively image materials at microwave frequencies, and to measure the local resistivity variations of semiconducting materials [2-5]. Fig. 1 shows a schematic illustration of our apparatus [6]. An open-ended coaxial cable is scanned just above the surface of a sample. In passive imaging mode, the microwave signal from the source is transmitted down the coaxial cable, reflected from the open end, and detected. At close separation between probe and sample, the reflected signal is strongly influenced by the conductivity of the sample. In active imaging mode, the microwave signal is applied to the device, and stray emissions are picked up by the scanning probe and detected. To construct an image, a computer controls the position of the sample and records the detector output as a function of position. In addition, one can measure either the magnitude of the signal, or the phase, using a microwave mixer.

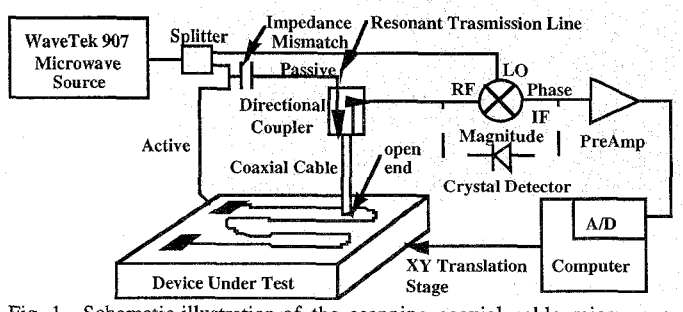

Fig. 1 Schematic illustration of the scanning coaxial cable microwave microscope.

The device under test is supported on an x-y translation stage by a manual z-axis translation stage and a two-axis leveling assembly. The sample can be scanned either at room temperature or in a liquid nitrogen bath. As will be discussed below, it was found that coupling the probe to a resonant section of transmission line significantly improved the sensitivity of the microscope. For this purpose, we have created a fixed impedance mismatch which is placed between the source and the directional coupler in both passive and active imaging modes (see Fig. 1).

III. Microscope Systematics

A. Spatial Resolution

The spatial resolution of the system is determined by the diameter of the inner conductor of the coaxial cable. To illustrate this, Fig. 2 shows a series of images of the NIST resolution target taken at the same probe/sample separation and frequency, using coaxial cables with different inner conductor dimensions. One sees that the images become sharper as the inner conductor diameter decreases. Quantitative measurements of the spatial resolution show that it is very nearly equal to the inner conductor diameter [6]. The 12 μm inner conductor probe has a spatial resolution of better than 20 μm when the inner conductor wire is dragged along the surface.

B. Contrast Mechanism

The contrast evident in Fig. 2 has several origins. Briefly, one can think of the coaxial cable inner conductor and the sample surface immediately below the inner conductor, as forming two plates of a parallel plate capacitor (we ignore the enhancement of the local electric field at the edges). As the separation between these two plates diminishes, the capacitance increases and more of the microwave signal in the cable is coupled to the sample. In the limit of close separation, the reflected signal from the

Manuscript received August 26, 1996.
This work was supported by the National Science Foundation through grant NSF ECS-9632811 and an NSF NYI grant DMR-9258183, and the Maryland Center for Superconductivity Research.

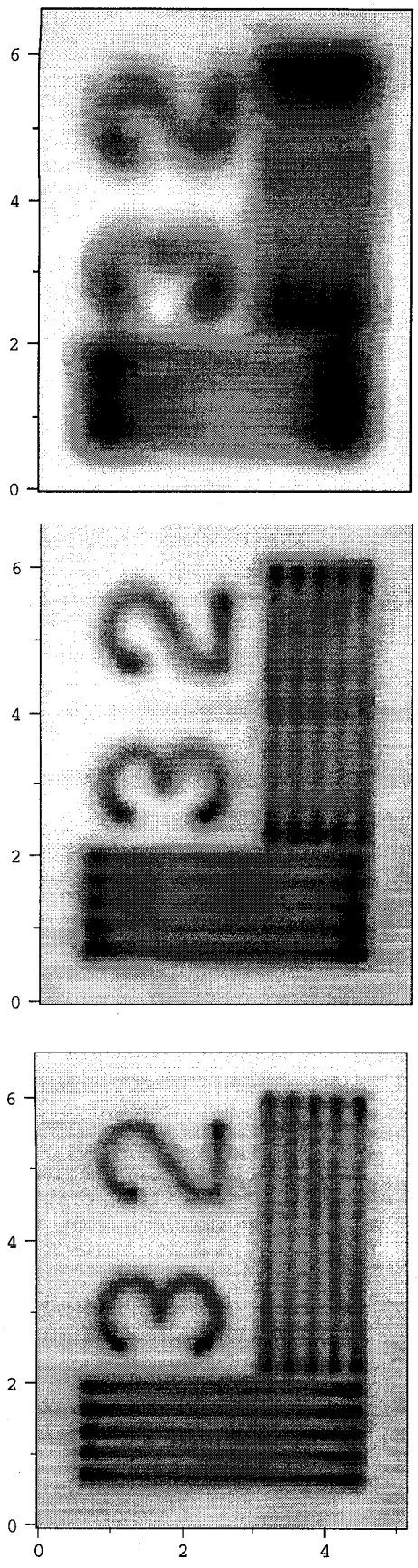

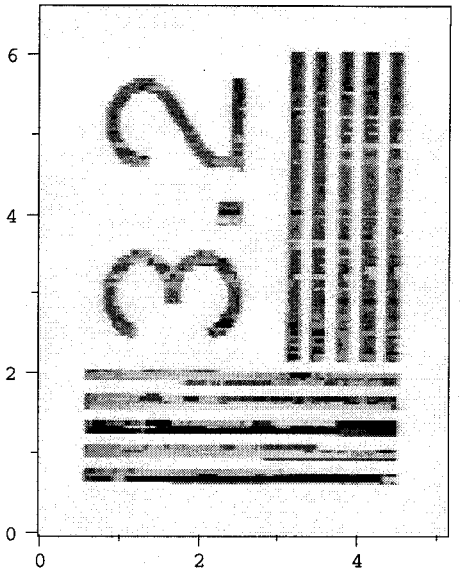

Fig. 2 Passive images of thin film Cr lines on a NIST resolution target taken at 11.7 GHz showing scans of the 3.2 lines / mm section. Images are taken with coaxial cable inner conductor sizes of top left) 480 μm, middle left) 200 μm, bottom left) 100 μm, and top right) 12 μm. The axes are distances in mm.

open end of the cable is very sensitive to the conductivity of the sample in the area immediately below the inner conductor.

A detailed model of this situation was presented in Ref. [6]. There, it was shown that the contrast sensitivity was increased by the existence of resonant standing wave modes on the coaxial cable between the microwave source and the probe tip. By measuring at frequencies which correspond to these standing wave conditions, one has enhanced sensitivity to the load presented by the sample. We have since inserted a deliberate impedance mismatch into our measurement system (Fig. 1) to enhance the standing waves.

Fig. 3 shows two passive mode frequency scans taken at different heights above a Cu microstrip circuit. Note that the reflected signal is periodic in frequency, with a periodicity corresponding to standing waves on a transmission line approximately 1 meter long with relative dielectric constant $\varepsilon_r = 1.3$. This length corresponds closely to the cable length between the fixed impedance mismatch and the probe tip (see Fig. 1). As the probe approaches the sample surface three things happen: the frequency of the resonant modes shift down, the quality factor of the resonances decrease, and the

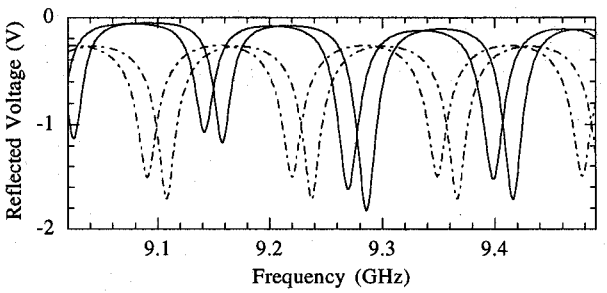

Fig. 3 Passive mode frequency scans (solid) at two heights above a Cu microstrip showing change in frequency, amplitude, and quality factor with probe/sample separation. The right trace was taken at 150 μm separation, while the left trace was taken at approximately 50 μm separation. The dot-dashed lines show results of the model discussed in the text, and have been offset from the data for clarity.

amplitude of the response changes. In principle, any of these effects can be used to create contrast for an image. The images presented in this paper are generated using the change in magnitude of the reflected signal at a fixed frequency. More sophisticated imaging schemes based on the frequency shift and change in quality factor are currently under development.

C. Loss Measurements

One can quantitatively determine the quality factors (Q) of the standing wave resonances shown in Fig. 3, and compare their values when the probe is either far or near the sample surface. Far from the sample the Q values are approximately 490, while closer they drop to approximately 448. One can extend the model given in [6] by adding a resistive load to the sample, R_x. One can fit the data in Fig. 3 at 150 μm separation using parameters $Z_s = 8\ \Omega$, $Z_0 = 50\ \Omega$ (source and line impedances), transmission line resonator length of 1.01 m, and $R_x = 0\ \Omega$ [6]. At close separation, one requires a height of 10 μm to produce the observed frequency shift (17.5 MHz), and $R_x = 5\ \Omega$ to produce the observed drop in Q. The model results are shown in Fig. 3 as dashed lines, and this demonstrates that the scanning coaxial probe microscope is sensitive to losses in the sample.

IV. Images

To be certain that the system is working properly before imaging cryogenic samples, we first imaged a series of test samples. These images also demonstrate the power and versatility of our microscope. Fig. 4 shows a photograph of a microstrip transmission line circuit, with two microstrip-to-coaxial connector feedthroughs just outside the photograph on the extreme left and right sides of the image. Fig. 5 is a passive microwave image taken at low resolution of the central part of the circuit, showing clearly the via holes and three separate conductors. Fig. 6 is an active image of the same circuit, taken over the same area as in Fig. 5. A microwave signal is applied to the connector on the left, while the connector on the right side of the package was left open. A clear standing wave pattern on the center conductor is visible in the image, taken at 8.01 GHz.

As discussed below, it is clear that active imaging is primarily sensitive to the voltage standing wave. The voltage standing wave pattern expected from a semi-infinite

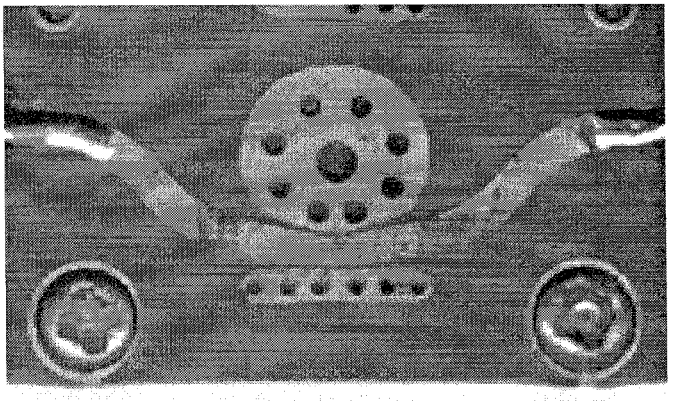

Fig. 4 Photograph of microstrip breadboard showing U-shaped circuit from feedthrough on the left to feedthrough on the right. The horizontal and vertical scales are 29 mm and 15 mm, respectively, and the total length of the microstrip shown is approximately 35 mm.

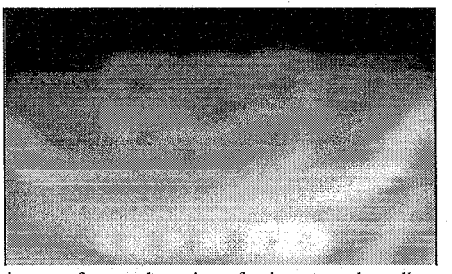

Fig. 5 Passive image of central section of microwave breadboard shown in Fig. 4, taken at 8.01 GHz with a 100 μm inner conductor coaxial probe. The scan area is 10 mm by 16 mm.

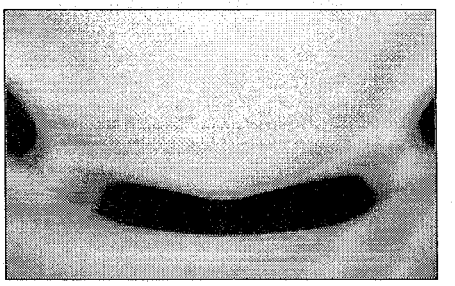

Fig. 6 Active image of microstrip breadboard shown in Fig. 4 taken at 8.01 GHz with a 100 μm inner conductor coaxial probe. The device is excited with a microwave signal on the left, and is terminated with an open on the right. The scan area is 10 mm by 15 mm, and the dark areas represent the strongest signal.

transmission line with an open termination at z = 0 is [7];

$$V(z) = 2\ V_0\ \cos\{2\pi z \varepsilon_r^{1/2}/\lambda\}$$

where it is assumed that a simple harmonic wave with free space wavelength λ and voltage V_0 is propagating down a transmission line with effective relative dielectric constant ε_r. From the spacing between the voltage nodes in Fig. 6 (13.5 mm), one can deduce that the effective dielectric constant of the microstrip transmission line shown in Fig. 4 is approximately $\varepsilon_r = 1.92$.

Fig. 7 is a photograph of a short microstrip transmission line lithographically defined on a two-sided copper printed circuit board. The strip is approximately 1 mm wide, the dielectric is 0.5 mm thick, and the microstrip terminates in an open on the right hand edge of the board.

Fig. 8 shows three active mode images of the microstrip taken at 8.03, 9.66 and 11.29 GHz with a signal applied by the coaxial cable on the left. In each case there is a maximum signal on the right hand side at the position of the

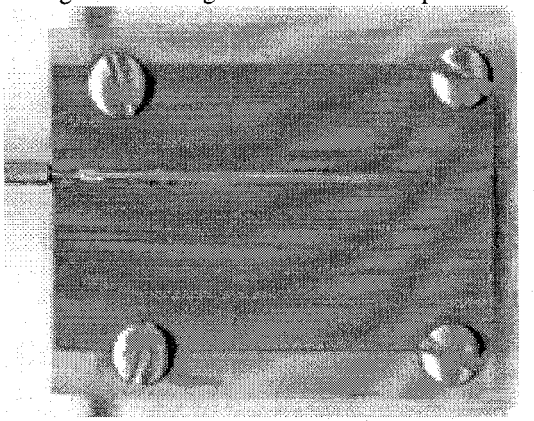

Fig. 7 Copper microstrip circuit showing coax-to-microstrip transition on left, and open circuit termination on right. The printed circuit board is 39 mm long and 33 mm wide, and the line is approximately 1 mm wide.

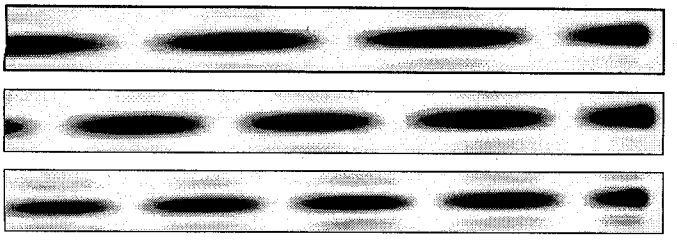

Fig. 8 Active images of copper microstrip shown in Fig. 7 with standing waves. Operating frequencies are (from top to bottom) 8.03 GHz, 9.66 GHz, and 11.29 GHz. The open end of the microstrip in on the right. The horizontal scale is 32.5 mm and the vertical scale on each panel is 3 mm.

open termination, leading us to conclude that the microscope is sensitive to voltage rather than current. A clear standing wave pattern is seen in each image, with a wavelength which decreases linearly with increasing frequency. Analysis of the three images gives effective dielectric constants for the printed circuit board microstrip in the range of 3.32 to 3.46.

Fig. 9 is a passive image of a $YBa_2Cu_3O_{7-\delta}$ (YBCO) thin film microstrip resonator taken at 12.0 GHz and room temperature. There is clear contrast between the 200 nm thick YBCO film and the 0.5 mm thick $LaAlO_3$ substrate. Fig. 10 shows an active mode image taken at 10.14 GHz in one of the resonant modes of the superconducting microstrip resonator. In this case, the resonator was at 77 K in a liquid nitrogen bath. The signal line of the microstrip is the YBCO film, while the ground plane is copper. This device, with a 500 μm wide inner conductor, is approximately 4 cm long, and has a fundamental resonance at approximately 1 GHz. A signal was applied to the device with a bared center conductor coaxial cable over the top pad shown in Fig. 9. The fields associated with this coupling method strongly contaminate the image in the vicinity of that pad, hence the image in Fig. 10 shows only the bottom part of the resonator. However,

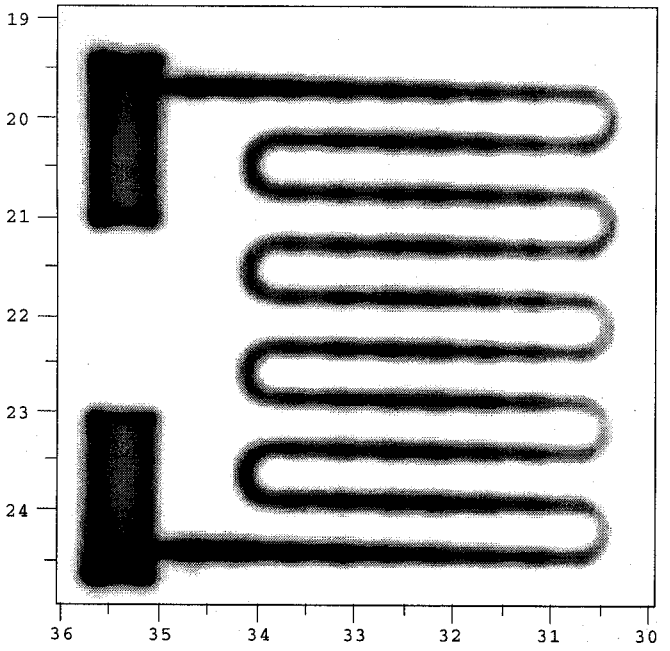

Fig. 9 Passive image taken at 12.0 GHz of a YBCO thin film microstrip circuit. The image was made at room temperature with a 100 μm inner conductor coaxial probe, and a probe/sample separation of approximately 50 μm. Distances are in mm.

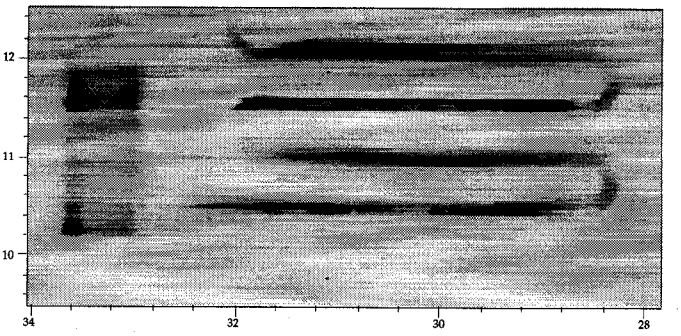

Fig. 10 Active image of YBCO resonator shown in Fig. 9 at 10.14 GHz in liquid nitrogen with the 100 μm coaxial probe. Distances are in mm.

one can see that voltage nodes and anti-nodes are sequentially arranged along the length of the YBCO microstrip. Because the interaction of the signals on neighboring lines may be significant, there is not a simple standing wave pattern present as in Figs. 6 and 8. However, one can estimate that there are approximately 5 full wavelengths present on the device at this frequency, corresponding to a mode number of 10, as expected.

V. Conclusions

We have demonstrated a simple and effective microwave imaging system which allows one to image the passive response of a material to microwave fields, as well actively measure the fields emitted by a high frequency circuit. The technique has nearly continuous frequency coverage, and has a spatial resolution which is limited by the diameter of a center conductor wire in a coaxial probe (currently 20 μm or less). The technique can image objects and circuits at room temperature, or in a liquid nitrogen bath, permitting the examination of superconducting microwave devices in their natural operating state.

Acknowledgment

We have benefited greatly from the work of Randy C. Black and Ajay Amar. We also thank Chang-Beom Eom and Brian Straughn for YBCO sample preparation.

References

[1] E. A. Ash and G. Nicholls, "Super-resolution Aperture Scanning Microscope," Nature vol. 237, pp. 510-512 (1972).

[2] C. A. Bryant and J. B. Gunn, "Noncontact Technique for the Local Measurement of Semiconductor Resistivity," Rev. Sci. Instrum. vol. 36, pp. 1614-1617 (1965).

[3] M. Fee, S. Chu and T. W. Hänsch, "Scanning Electromagnetic Transmission Line Microscope with Sub-Wavelength Resolution," Optics Commun. vol. 69, pp. 219-224 (1989).

[4] T. Wei, X. D. Xiang, W. G. Wallace-Freedman, and P. G. Schultz, "Scanning Tip Microwave Near-Field Microscope," Appl. Phys. Lett. vol. 68, pp. 3506-3508 (1996).

[5] M. Golosovsky and D. Davidov, "Novel Millimeter-Wave Near-Field Resistivity Microscope," Appl. Phys. Lett. vol. 68, pp. 1579-1581 (1996).

[6] C. P. Vlahacos, R. C. Black, S. M. Anlage, A. Amar, and F. C. Wellstood, "Near-Field Scanning Microwave Microscope with 100 μm Resolution," Appl. Phys. Lett. (in press, 1996).

[7] S. Ramo, J. R. Whinnery, and T. Van Duzer, Fields and Waves in Communication Electronics, (J. Wiley, New York, 1984), page 238.